Supplementary Materials

Effect of the heterovalent doping of TiO_2 with Sc^{3+} and Nb^{5+} on the defect distribution and photocatalytic activity

Petr D. Murzin, Aida V. Rudakova, Alexei V. Emeline, Detlef W. Bahnemann*

Laboratory "Photoactive Nanocomposite Materials", Saint-Petersburg State University, Saint-Petersburg, Russia

* detlef.bahnemann@spbu.ru

Photoinduced defect formation

In its simplified scenario, the mechanism of photostimulated defect formation can be represented as follows:

1. $TiO_2 + h\nu \rightarrow e + h$
2. $D_e + e \rightarrow D_e^-$ p
3. $D_e^- + h \rightarrow D_e$ q

Here, the first step describes the photoexcitation of TiO_2, the second step corresponds to the electron trapping by pre-existing defects, D_e, with a probability p, leading to the formation of photoinduced defects, D_e^-, and the third step describes a decay of photoinduced defects with a probability q, due to recombination with charge carriers of the opposite charge.

The solution of the corresponding kinetic equations results in the following expression describing the kinetics of photoinduced defects' accumulation:

$$D_e^-(t) = N_0\left(\frac{p}{p+q}\right) + \left(D_0 - N_0\left(\frac{p}{p+q}\right)\right) \cdot e^{-t/\tau} \quad \text{(S1)}$$

here, D_0 and N_0 are the concentrations of pre-existing defects with trapped charge carriers before irradiation and the total concentration of defect states of both types (with and without trapped charge carriers), respectively, and τ is the characteristic time of defect formation:

$$\tau = 1/(p+q) \quad \text{(S2)}$$

According to Equation (S1), at a sufficiently long irradiation time, the number of photoinduced defects is approaching to the limit:

$$D_{e\,\infty}^- = N_0\left(\frac{p}{p+q}\right) \quad \text{(S3)}$$

In our experiments on photoinduced defect formation, the limit was achieved within 15 minutes of UV irradiation.

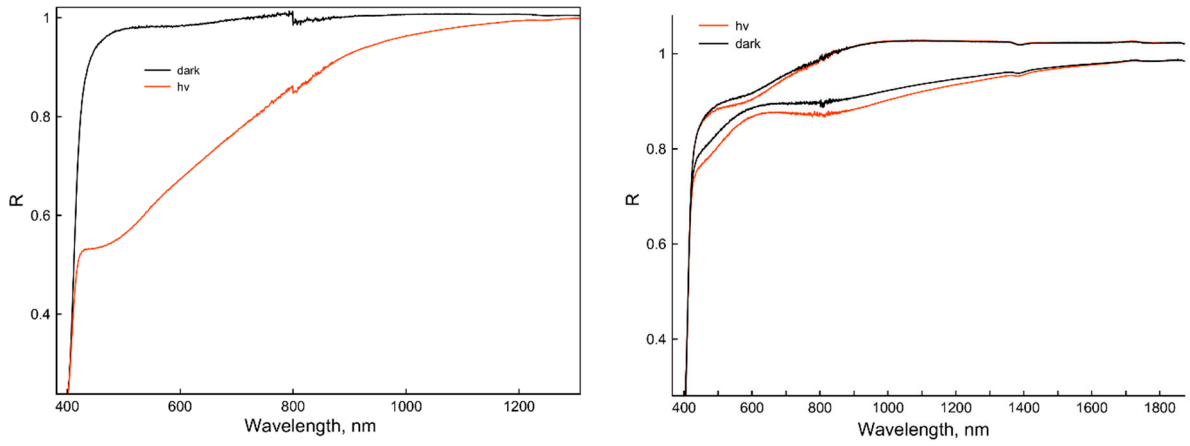

(a) **(b)**

Figure S1. Diffuse reflectance spectra before and after UV irradiation of doped TiO_2: **(a)** Sc-doped (0.1 at.% Sc) TiO_2, and **(b)** TiO_2 (top pair of spectra) and Nb-doped (0.74 at.%) TiO_2 (bottom pair of spectra).

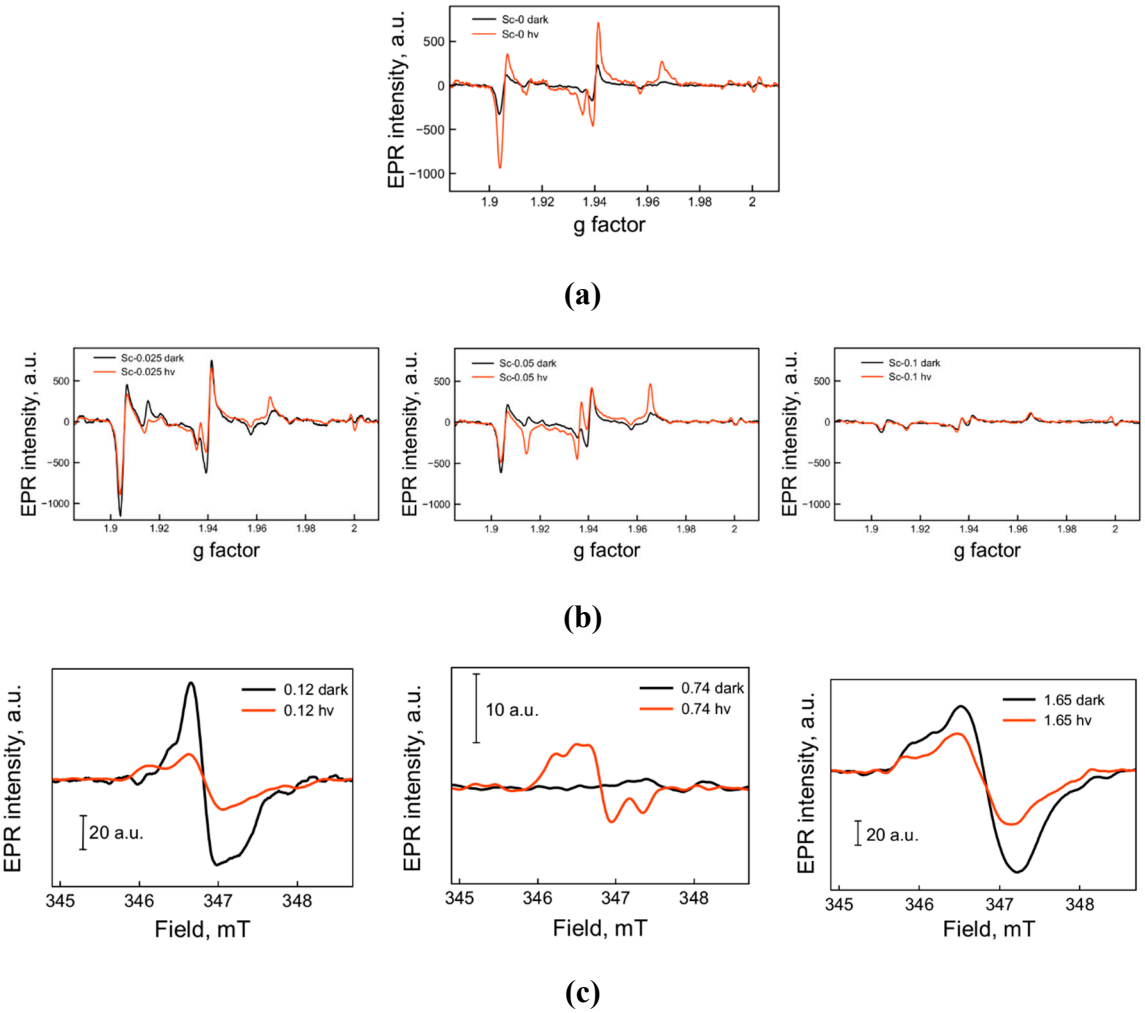

(a)

(b)

(c)

Figure S2. EPR spectra of **(a)** pristine and **(b)** Sc^{3+}- and **(c)** Nb^{5+}-doped TiO_2.

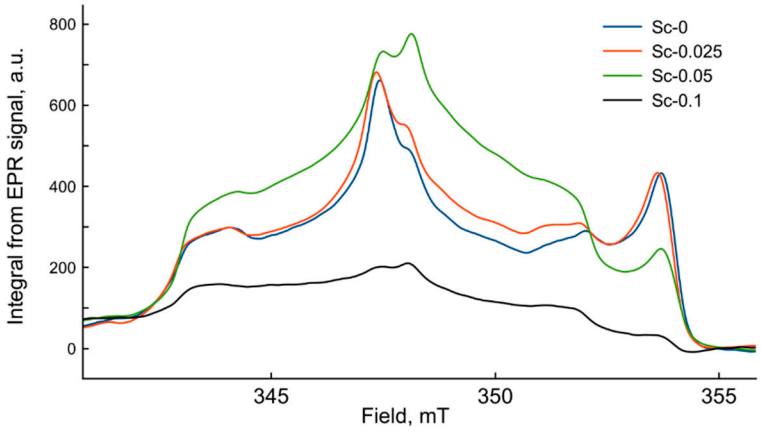

Figure S3. Integrated EPR spectra of Sc-doped TiO_2.

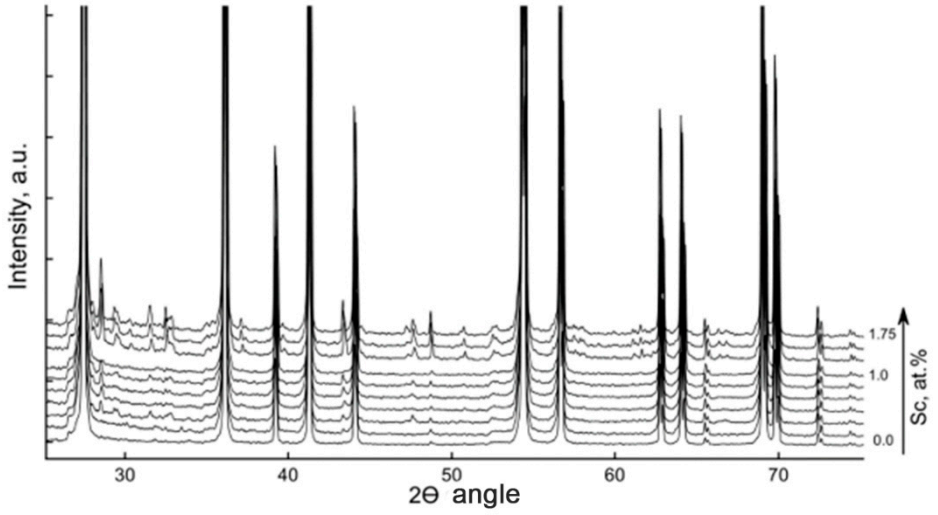

(a)

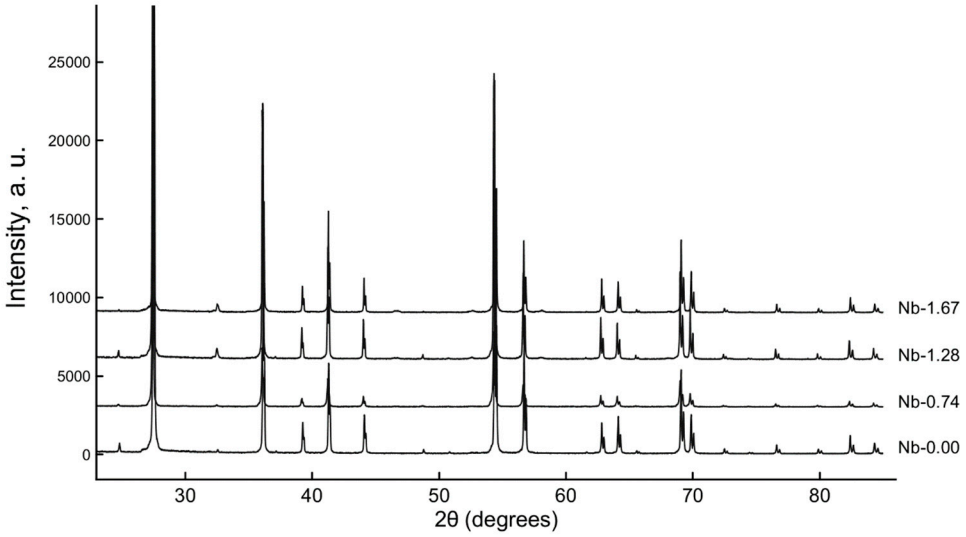

(b)

Figure S4. XRD pattern of **(a)** Sc-doped TiO_2 and **(b)** Nb-doped TiO_2.

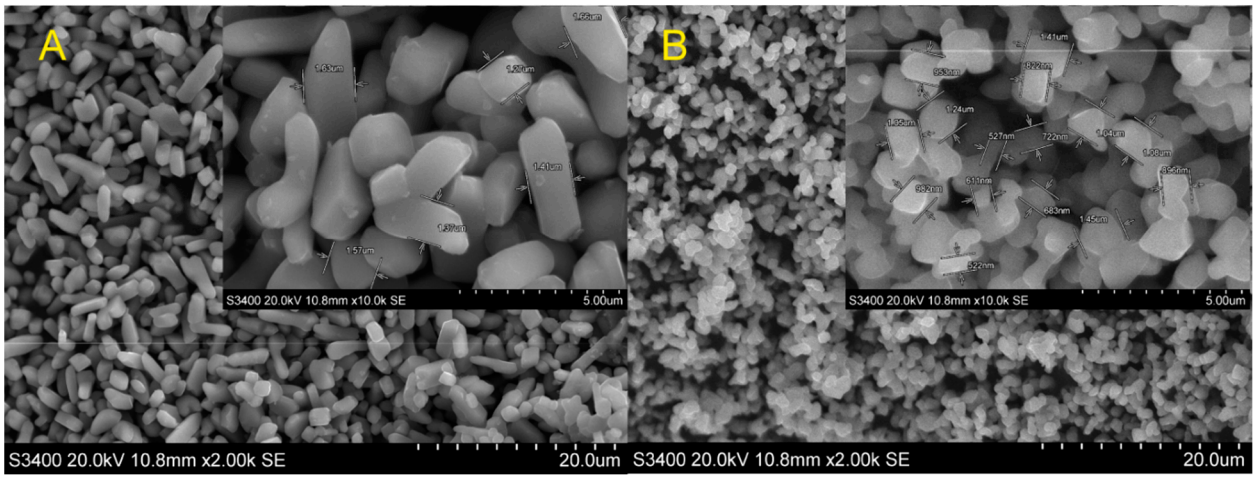

(a) **(b)**

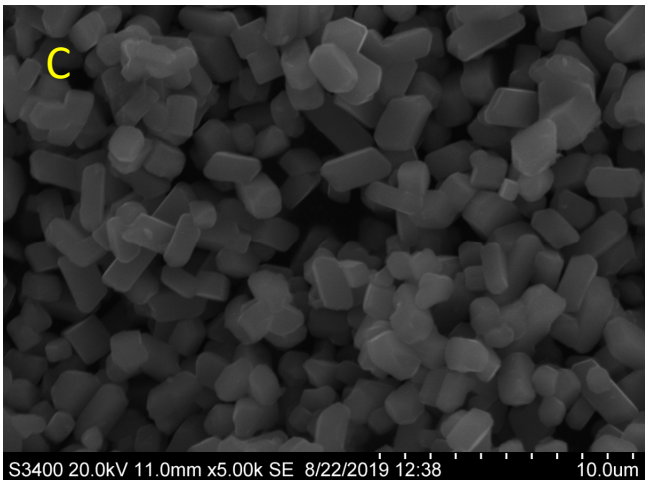

(c)

Figure S5. Electron microscopic images of **(a)** undoped TiO_2, **(b)** Nb-doped TiO_2, and **(c)** Sc-doped TiO_2.

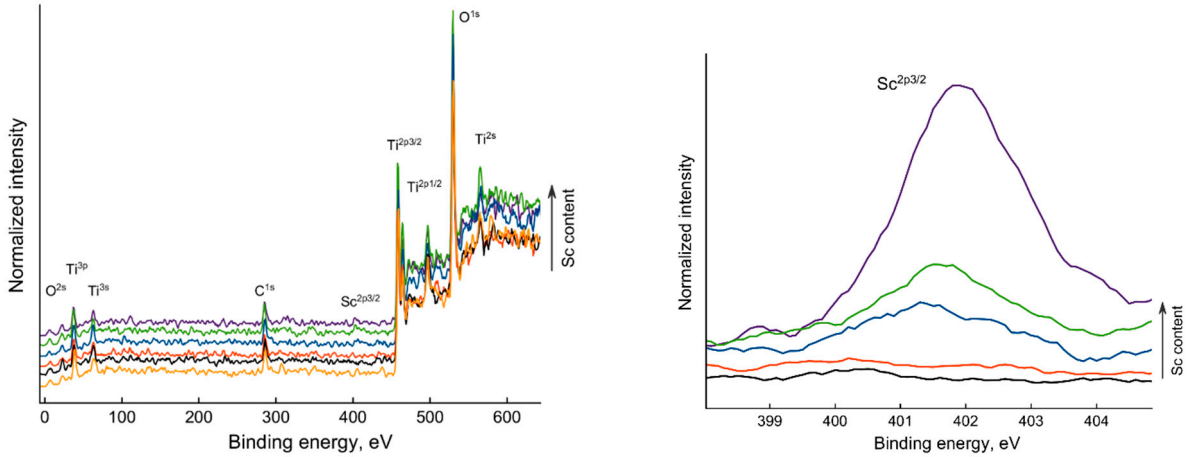

(a)

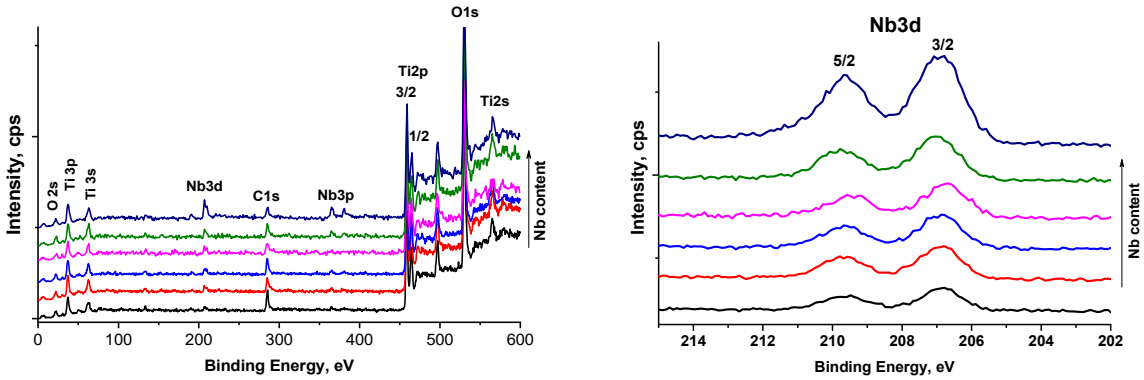

(b)

Figure S6. XPS spectra of **(a)** Sc-doped TiO_2 and **(b)** Nb-doped TiO_2.

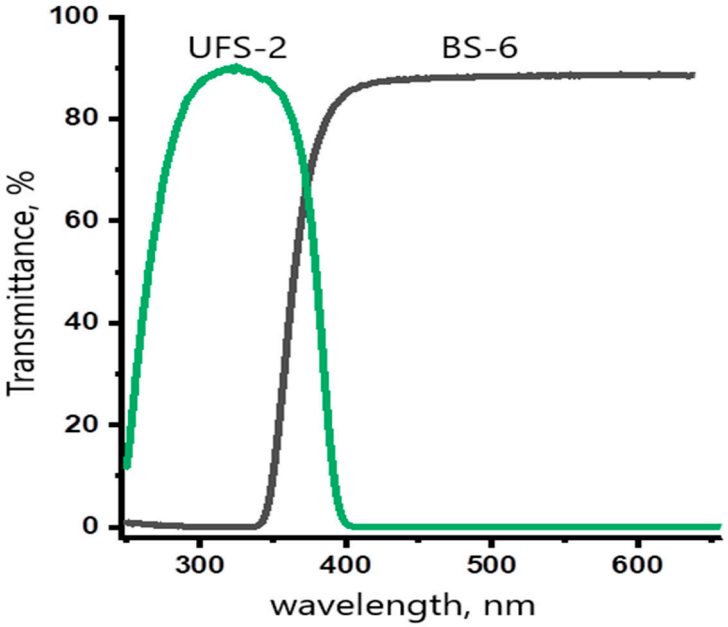

Figure S7. Transmittance spectra of BS-6 cut-off and UFS-2 bandpass filters.

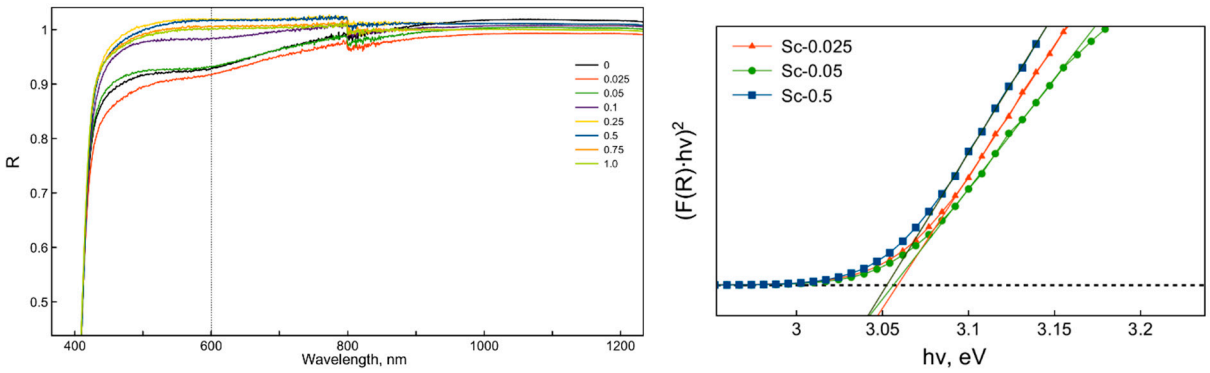

(a)

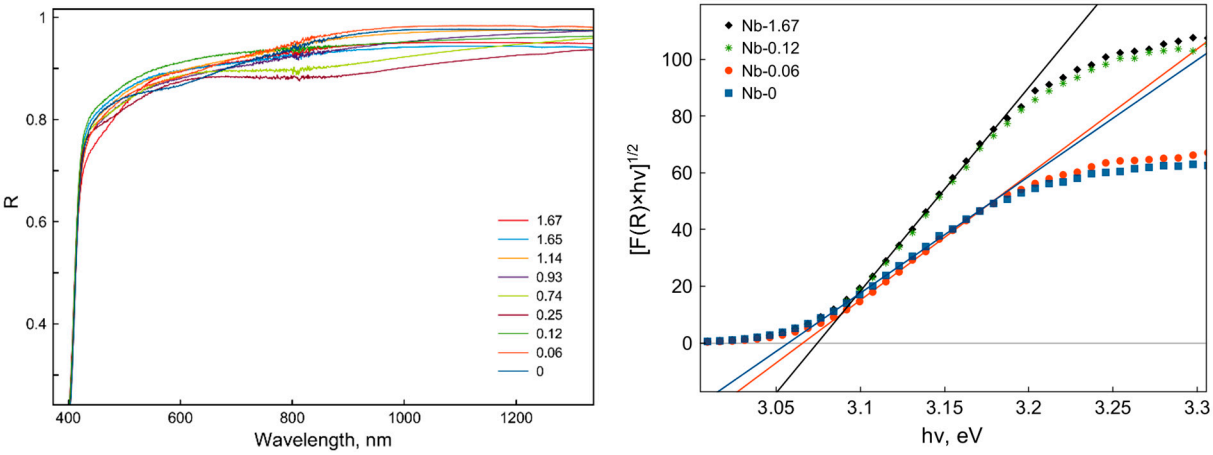

(b)

Figure S8. Diffuse reflectance spectra and Tauc plot transformation for **(a)** Sc-doped and **(b)** Nb-doped TiO_2 samples.